

# Diagnostic of Cystic Fibrosis in Lung Computer Tomographic Images using Image Annotation and Improved PSPNet Modelling

N J Francis<sup>1</sup>, N S Francis<sup>1</sup>, S V Axyonov<sup>1</sup>, S A Aljarar<sup>2</sup>, Y Xu<sup>2</sup> and M Saqib<sup>3</sup>

<sup>1</sup>Engineering School of Information Technology and Robotics, Tomsk Polytechnic University, Lenin Avenue, 30, Tomsk, 634034, Russia

<sup>2</sup>School of Nuclear Science and Engineering, Tomsk Polytechnic University, Lenin Avenue, 30, Tomsk, 634034, Russia

<sup>3</sup>Research School of Chemistry and Applied Biomedical Sciences, Tomsk Polytechnic University, Lenin Avenue, 30, Tomsk, 634034, Russia

E-mail : natzina\_92@yahoo.com

**Abstract.** The research deals with the development of an algorithm for detecting pathological formation in cystic fibrosis using the PSPNet model with focal loss. The model allows data sets to be entered in accordance to their similarities based on their pathological diagnostic signs. The simple and effective algorithm structure groups annotated images, processes them in a multi-scale CNN, and localizes areas of cystic fibrosis in the lungs with high accuracy.

## 1. Introduction

Cystic Fibrosis (CF) [1, 2] is a hereditary condition, where excess mucous produced in the lungs leads to various respiratory diseases. A patient suffering from CF is prone to it for life, as there is no cure for this life-threatening disease. Pneumonia and Bronchitis are commonly known diseases that occur in patients with CF. Hence, detecting the disease at an early stage plays a vital role in reducing the impact that CF has on the patient.

The proposed CAD system will assist radiologists to accurately detect CF in lung computer tomography (CT) images. The CT images which are identified with CF can also be used for future research purposes in the medical and computational fields. Hence, the research concentrates on producing accurate outputs that aid in increasing various therapeutic options to detect CF at an early stage.

The pyramid scene parsing network (PSPNet) [3] has displayed accuracy in the high computational segmentation [4, 5] of the brain. The multiple scaling process [6] refines the accuracy of the detection before being upsampled to the original image size. Hence, the PSPNet will also positively aid in the detection of CF in lung CT images.

An ongoing experiment to detect pulmonary fibrosis in lung CT images is possible by subjectively dividing high-resolution computer tomography images (HRCT) [7] into various subsets before training the dataset. Since CT images of CF may contain a number of variations, the process of dividing them accordingly should be taken into account to display accurate results. The algorithm is simple and is developed to focus purely on pathologies occurred through CF rather than CT images as a whole.



The purpose of the study is to create a computational model that annotates images according to their pathologies, and to detect CF from the annotated images using an improved PSPNet model with accuracy.

**2. Methods and Technologies**

The process for detecting CF is carried out in two simple stages:

- Categorize the input, which are the HRCT images according to their similarities
- Identify CF.

*2.1. Categorize the Input, which are the HRCT Images According to their Similarities*

In this stage, HRCT images are collectively input into the system. The images are annotated and trained by a multi-scale CNN [8, 9]. This process of feature extraction [10] and pixel manipulation [11] helps identify detailing in images, and image outputs are automatically grouped according to their similarities into a number of subsets.

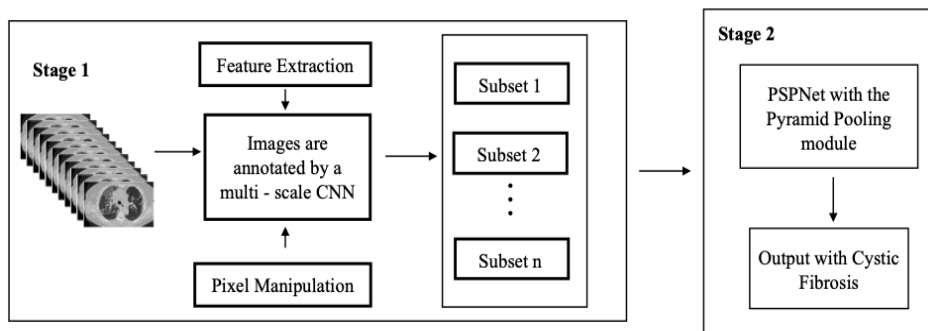


**Figure 1.** Structural working of the system in two stages:  
 Stage 1 - HRCT images annotated using a multi-scale CNN,  
 Stage 2 - PSPNet with the pyramid module for identifying CF.

*2.2. Identify CF*

In this stage, the image subsets are passed via PSPNet with the pyramid pooling module. This region based contextual aggregation is known in the pyramid pooling module [12], where images are inputted at various scales.

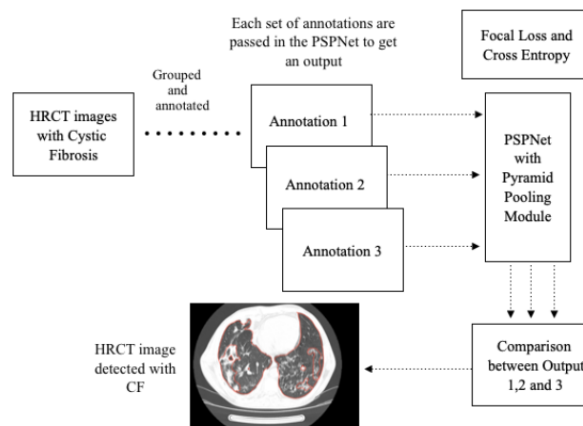


**Figure 2.** An individual subset consisting of annotated images to be passed into the PSPNet.

In Figure 2, images that are annotated and passed into the second phase with the PSPNet as depicted.

In the feature map [13] of the pyramid module, the final network layer indicates the use of pooling kernels [14]. CF cysts are identified by taking into account the final layer of the convolutional network which consists of a feature that is obtained from the feature map. Average pooling [15] is applied to the element that is identified in the feature map. The feature map sizes, which are actually the output of the average pooling that is applied to the feature map, are divided into sizes 1×1, 2×2 and so on. The final output of the pyramid module is achieved by applying a 1×1 convolution neural network (CNN) to every feature map. The image is restored to the original size with equal weights by Upsampling and Bilinear Interpolation [16]. By this process, the final feature map is restored to the required dimension. Finally, the final layer of the feature map that is input into the system is concatenated with the previously obtained feature map to produce the required output.

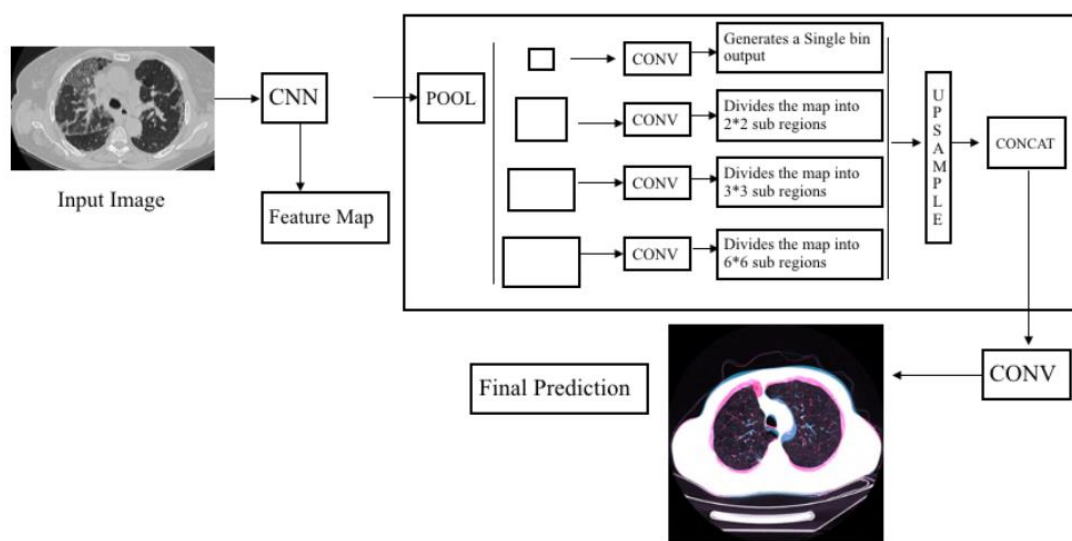


**Figure 3.** PSPNet incorporated with the pyramid pooling module to detect CF.

In Figure 3, the process of the pyramid pooling module with the PSPNet is depicted in detail. The input CT image is convolved to four scales before it is upsampled and concatenated to produce the original image.

The pre-processing techniques in the network incorporates functions to deal with mucous distortion or pathologies as seen in the CT images containing CF that is input into the system. Fuzzy logic technique is implied to detect mucous, and the Binary Image morphing technique helps to detect blood vessels and veins which differentiate them from pathologies. Finally, focal loss [17] and cross entropy [17] techniques are used to focus on all less confidently classified classes. This reduces the loss obtained in the final output.

The focal loss is derived using the equation:

$$fc(m,n) = -n(1-m)\gamma\log(m) - (1-n)m\gamma\log(1-m)$$

where,  $fc$  is the focal loss, and  $\gamma$  is the respective down weights in the classified samples.

The cross-entropy loss is derived using the equation:

$$e(a,b) = -t\log(a) - (1-t)(1-b)\log(1-a)$$

where,  $e$  is the cross-entropy loss, and  $t$  is the weights.

The focal loss in the PSPNet is denoted by  $\gamma=1$ , which increases the performance of the model. The final output is derived by a comparative analysis. The images that are annotated a number of times as seen in figure 2, are input into the system with the PSPNet combined with the pyramid module. After the image is processed and trained to detect CF, a certainty in the results is obtained by passing the

output of the PSPNet through a basic image comparison process. The final output thus accurately displays the image with CF.

**3. Experimental analysis and results**

The training data set consists of 312 HRCT images that were obtained from local hospitals. The data, after passing through the first stage of training, was reported to contain 128 CF patients. Out of the 128 affected patients, 71 were detected as female CT images, and 57 were detected as male CT images. The Kruskal-Wallis test was performed to determine the statistical performance of the model.

The CT image annotated via CAD displayed better competence in producing results. A comparison between variables that displayed continuity and dichotomy was performed to analyse the output produced. Testing was carried out on 5 test case samples for 42 complete epochs. Each test case sample consisted of approximately 63 CT images. The overall p-value was calculated as 0.00757. Table 1 below displays the accuracy of similarity by a comparative analysis between four selected pathologies (P1, P2, P3 and P4) respectively. The similarity median is first calculated for each pathology separately, then a pathology pair (for example, P1:P2) is formed by taking the higher median values of the four medians analysed, from which the average median value was calculated and displayed in the table. The difference in similarity of the pathologies for each test case is given by their P-value below:

**Table 1.** Kruskal-Wallis performance analysis

Pathologies	Median	Quarter Epoch Cycle	Mid Epoch Cycle	P-Value
<b>P1:P2 vs P1:P3</b>	40.32	16.84	66.89	0.00757
<b>P1:P2 vs P1:P4</b>	4.87	1.45	15.85	0.01630
<b>P1:P3 vs P1:P4</b>	24.58	10.54	54.12	0.00938
<b>P2:P3 vs P1:P2</b>	40.36	16.87	66.91	0.00143
<b>P2:P3 vs P1:P3</b>	3.56	1.02	15.72	0.01484
<b>P2:P3 vs P1:P4</b>	24.58	10.54	54.12	0.00974
<b>P2:P4 vs P1:P2</b>	40.32	16.84	66.89	0.01024
<b>P2:P4 vs P1:P3</b>	4.87	1.45	15.85	0.00934
<b>P2:P4 vs P1:P4</b>	24.62	10.57	54.17	0.00998
<b>P3:P4 vs P1:P2</b>	6.81	2.83	14.73	0.01005
<b>P3:P4 vs P1:P3</b>	40.44	16.91	66.94	0.00743
<b>P3:P4 vs P1:P4</b>	5.06	1.53	15.04	0.00938
<b>P3:P4 vs P2:P4</b>	8.11	3.11	14.22	0.00699
<b>P2:P3 vs P2:P4</b>	4.87	1.45	15.85	0.01018
<b>P2:P3 vs P3:P4</b>	40.33	16.88	66.92	0.00871

To decipher the difference in similarity in the four pathologies that were tested, H-statistics (H) is calculated:

$$H = (12/N(N+1)) \cdot (\sum T^2/n) - 3(N+1) = 0.018 \cdot 5612.7 - 78 = 23.0286 \text{ and } p\text{-value} < 0.01$$

Where the value of N represents the number of data samples per test (N = 25, n = 5) and T is the ranks set to all images within the data samples according to accuracy in their similarities.

The invariant annotation of images without the use of a CAD system shows inconsistency. It usually requires an expert to correct any missed regions during the annotation.

**Table 2.** Output performance with/without annotated CT images using the CAD System

Experimental Analysis	F1 Score (Manual)	F1 Score (CAD)
<b>Test Case 1</b>	0.8730	0.9091

<b>Test Case 2</b>	0.8353	0.9061
<b>Test Case 3</b>	0.9490	0.9764
<b>Test Case 4</b>	0.7819	0.8361
<b>Test Case 5</b>	0.8550	0.9035

The competency of the output is statistically analysed by evaluating the accuracy rate depending on the number of false positives and false negatives. The Sensitivity (TPR) and Specificity (SP) of the detected CF in CT images is 0.8366 and 0.9436 respectively. Based on the TPR and SP values, the precision is calculated to 0.9209, thus infirming that the negative predictive value for the detected CF is about 0.8804. The false positive and negative rate is 0.0564 and 0.1634. The false discovery rate is 0.0791 based on the percentage of FP and FN, with an accuracy rate of 0.8966. The F1 score that balances the precision with the accuracy obtained is 0.8767. The overall working performance of the model based on the output and quality obtained is determined by Mathew’s Correlation Coefficient, which is an approximate of 0.7906.

Figure 4 displays the graphical analysis of the overall system performance. In Figure 4(a), the system is analyzed for every training cycle where sensitivity and specificity are calculated to check the number of false positives and negatives. Increase in sensitivity and specificity depicts lesser false positive and negative values. Figure 4(b) calculates the error rate for all 5 test cases in terms of its probability. According to data acquired from the graph, the probability of error lies between 0 and 0.25, which proves the efficiency of the system in detecting CF.

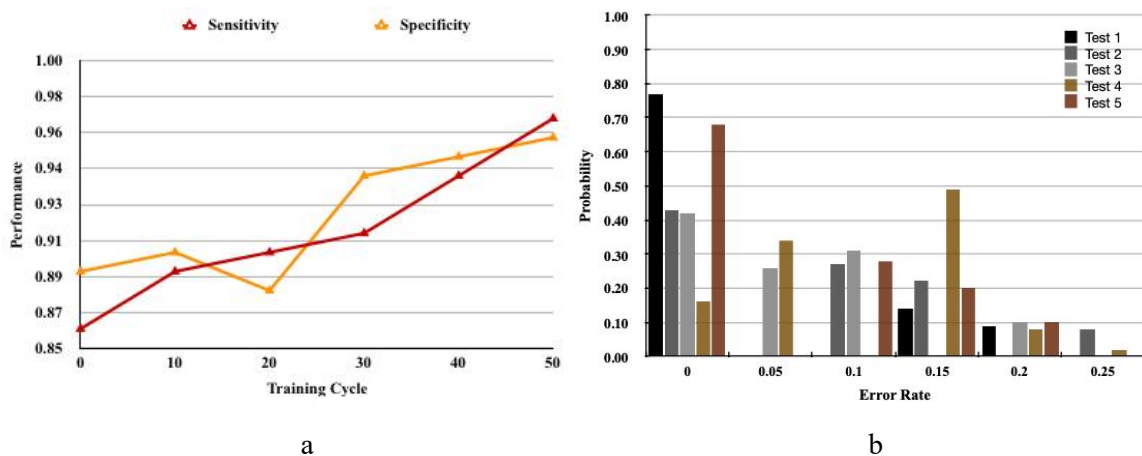


**Figure 4.** Graphical analysis: a) system output performance b) system error probability.

Thus, the overall statistical analysis displays the consistency of the working model. The model will be tested in future researches for various other diseases pertaining to lung CT images.

**4. Conclusion**

The collective input of datasets can create a variation during training. Hence, by the method of annotating CT images, and training them to be grouped according to similar pathologies, help in paving the way for successful identifications of Cystic Fibrosis. The number of subsets that are obtained can be passed via PSPNet with the pyramid pooling module. Multiple scaling techniques in the pooling module help to scale and successfully identify pathologies related to Cystic Fibrosis. This model is efficient and displays accuracy in the detection of CF.

This model can also aid in future researches, to identify lung CT images pertaining to deadlier diseases like COVID-19.

**References**

- [1] Mumcuoglu E U, Prescott J, Baker B N, et al. 2009 Image analysis for cystic fibrosis: automatic lung airway wall and vessel measurement on CT images. Conference Proceedings : Annual International Conference of the IEEE Engineering in Medicine and Biology Society. *IEEE Engineering in Medicine and Biology Society. Annual Conference*. 2009 3545-48
- [2] Rosenow T, Oudraad M C, Murray C P, Turkovic L, Kuo W, de Bruijne M, Ranganathan S C, Tiddens H A & Stick S M 2015 PRAGMA-CF. A quantitative structural lung disease computed tomography outcome in young children with cystic fibrosis. *American journal of respiratory and critical care medicine* **191** (10) 1158-65
- [3] Zhao H, Shi J, Qi X, Wang X and Jia J 2017 Pyramid scene parsing network. In: *IEEE Conf. on Computer Vision and Pattern Recognition (CVPR)*, pp 2881-90
- [4] Lavanya M and Muthu K P 2017 Lung Lesion Detection in CT Scan Images Using the Fuzzy Local Information Cluster Means (FLICM) Automatic Segmentation Algorithm and Back Propagation Network Classification. *Asian Pac J Cancer Prev* **18** (12) 3395-99
- [5] Gang P, Zeng W, Gordienko Y, Kochura Y, et al. 2019 Effect of Data Augmentation and Lung Mask Segmentation for Automated Chest Radiograph Interpretation of Some Lung Diseases. *International Conference on Neural Information Processing*. pp 333-340
- [6] Liu X, Deng Z & Yang Y 2019 Recent progress in semantic image segmentation. *Artif Intell Rev* **52** 1089-06
- [7] Walsh S L F, Calandriello L, Silva M and Sverzellati N 2018 Deep learning for classifying fibrotic lung disease on high-resolution computed tomography: a case-cohort study. *Lancet Respir Med*. **6** (11) 837-845
- [8] Li S, Zhu X & Bao J 2019 Hierarchical Multi-Scale Convolutional Neural Networks for Hyperspectral Image Classification. *Sensors* **19** (7) 1714
- [9] Fisher Y and Koltun V 2016 Multi-Scale Context Aggregation by Dilated Convolutions. ICLR.
- [10] Zhao H and Liu H 2019 Multiple classifiers fusion and CNN feature extraction for handwritten digits recognition. *Granul. Comput.* **5** 411-418
- [11] Bianli D, Xiaokang R and Jie R 2019 CNN-based Image Super-Resolution and Deblurring. In Proceedings of the 2019 *International Conference on Video, Signal and Image Processing (VSIP 2019)*. Association for Computing Machinery, New York, NY, USA, 70-74. DOI:<https://doi.org/10.1145/3369318.3369328>.
- [12] He K, Zhang X, Ren S and Sun J 2014 Spatial Pyramid Pooling in Deep Convolutional Networks for Visual Recognition. *Lecture Notes in Computer Science* 346-361
- [13] Kim I, Rajaraman S & Antani S 2019 Visual Interpretation of Convolutional Neural Network Predictions in Classifying Medical Image Modalities. *Diagnostics* (Basel, Switzerland) **9** (2) 38
- [14] Hu W, Zhang Y & Li L 2019 Study of the Application of Deep Convolutional Neural Networks (CNNs) in Processing Sensor Data and Biomedical Images. *Sensors* **19** (16) 3584
- [15] Liu X, Zhou Q, Zhao J, Shen H & Xiong X 2019 Fault Diagnosis of Rotating Machinery under Noisy Environment Conditions Based on a 1-D Convolutional Autoencoder and 1-D Convolutional Neural Network. *Sensors* **19** (4) 972
- [16] Natzina Juanita S R F, et al. 2020 Analysis and Detection of Community Acquired Pneumonia Using PSPNET with Complex Daubechies Wavelets. *Indian Journal of Computer Science and Engineering* **11** (3) 217-226
- [17] Lin T Y, Goyal P, Girshick R, He K and Dolla P 2020 Focal loss for dense object detection. *IEEE transactions on pattern analysis and machine intelligence* **42** (2) 318-327